

## Distal deposition of tephra from the Eyjafjallajökull 2010 summit eruption

J. A. Stevenson,<sup>1</sup> S. Loughlin,<sup>2</sup> C. Rae,<sup>3</sup> T. Thordarson,<sup>1</sup> A. E. Milodowski,<sup>4</sup> J. S. Gilbert,<sup>5</sup> S. Harangi,<sup>6</sup> R. Lukács,<sup>6</sup> B. Højgaard,<sup>7</sup> U. Árting,<sup>7</sup> S. Pyne-O'Donnell,<sup>8</sup> A. MacLeod,<sup>9</sup> B. Whitney,<sup>10</sup> and M. Cassidy<sup>11</sup>

Received 23 September 2011; revised 11 April 2012; accepted 16 April 2012; published 6 June 2012.

[1] The 2010 Eyjafjallajökull lasted 39 days and had 4 different phases, of which the first and third (14–18 April and 5–6 May) were most intense. Most of this period was dominated by winds with a northerly component that carried tephra toward Europe, where it was deposited in a number of locations and was sampled by rain gauges or buckets, surface swabs, sticky-tape samples and air filtering. In the UK, tephra was collected from each of the Phases 1–3 with a combined range of latitudes spanning the length of the country. The modal grain size of tephra in the rain gauge samples was 25  $\mu\text{m}$ , but the largest grains were 100  $\mu\text{m}$  in diameter and highly vesicular. The mass loading was equivalent to 8–218 shards  $\text{cm}^{-2}$ , which is comparable to tephra layers from much larger past eruptions. Falling tephra was collected on sticky tape in the English Midlands on 19, 20 and 21st April (Phase 2), and was dominated by aggregate clasts (mean diameter 85  $\mu\text{m}$ , component grains <10  $\mu\text{m}$ ). SEM-EDS spectra for aggregate grains contained an extra peak for sulphur, when compared to control samples from the volcano, indicating that they were cemented by sulphur-rich minerals e.g. gypsum ( $\text{CaSO}_4 \cdot \text{H}_2\text{O}$ ). Air quality monitoring stations did not record fluctuations in hourly PM10 concentrations outside the normal range of variability during the eruption, but there was a small increase in 24-hour running mean concentration from 21–24 April (Phase 2). Deposition of tephra from Phase 2 in the UK indicates that transport of tephra from Iceland is possible even for small eruption plumes given suitable wind conditions. The presence of relatively coarse grains adds uncertainty to concentration estimates from air quality sensors, which are most sensitive to grain sizes <10  $\mu\text{m}$ . Elsewhere, tephra was collected from roofs and vehicles in the Faroe Islands (mean grain size 40  $\mu\text{m}$ , but 100  $\mu\text{m}$  common), from rainwater in Bergen in Norway (23–91  $\mu\text{m}$ ) and in air filters in Budapest, Hungary (2–6  $\mu\text{m}$ ). A map is presented summarizing these and other recently published examples of distal tephra deposition from the Eyjafjallajökull eruption. It demonstrates that most tephra deposited on mainland Europe was produced in the highly explosive Phase 1 and was carried there in 2–3 days.

**Citation:** Stevenson, J. A., et al. (2012), Distal deposition of tephra from the Eyjafjallajökull 2010 summit eruption, *J. Geophys. Res.*, 117, B00C10, doi:10.1029/2011JB008904.

### 1. Introduction

[2] Tephra deposition in Europe by Icelandic volcanoes is not uncommon. Swindles *et al.* [2011] published a review of tephras from the past 7000 years that were found in the Faroe Islands, Scandinavia, Great Britain, Ireland and Germany,

and estimated a 16% probability of an ash cloud reaching northern Europe in any given decade. This is likely to be a minimum estimate, as the evidence for older eruptions is limited to those large enough that their tephra can be recovered from soil and lake cores many years after the event, and because difficulties in recovering basaltic microtephras have

<sup>1</sup>School of Geosciences, Edinburgh University, Edinburgh, UK.

<sup>2</sup>British Geological Survey, Edinburgh, UK.

<sup>3</sup>AEA, Glengarnock Technology Centre, Glengarnock, UK.

<sup>4</sup>British Geological Survey, Keyworth, UK.

Corresponding author: J. A. Stevenson, School of Geosciences, Edinburgh University, Grant Institute, West Mains Road, Edinburgh EH9 3JW, UK. (john.stevenson@ed.ac.uk)

Copyright 2012 by the American Geophysical Union.  
0148-0227/12/2011JB008904

<sup>5</sup>Lancaster Environment Centre, Lancaster University, Lancaster, UK.

<sup>6</sup>Institute of Geography and Earth Sciences, Eötvös University Budapest (ELTE), Budapest, Hungary.

<sup>7</sup>Jarðfeingi, Tórshavn, Faroe Islands.

<sup>8</sup>Department of Earth Science, University of Bergen, Bergen, Norway.

<sup>9</sup>Department of Geography, University of London, Royal Holloway, Egham, UK.

<sup>10</sup>School of Geosciences, Edinburgh University, Edinburgh, UK.

<sup>11</sup>National Oceanography Centre, University of Southampton, Southampton, UK.

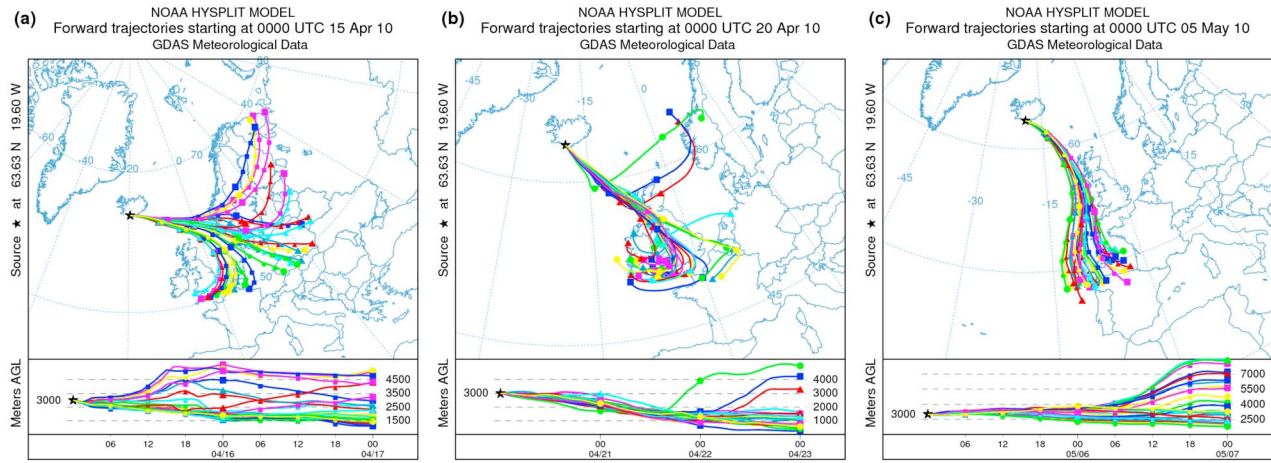


**Figure 1.** Maps of modeled particle trajectories, calculated with HYSPLIT ([http://ready.arl.noaa.gov/HYSPLIT\\_traj.php](http://ready.arl.noaa.gov/HYSPLIT_traj.php)). The plots are forward ensemble trajectory models using GDAS weather data. The different paths are produced by offsetting the meteorological data by one grid square in X, Y, or Z (27 combinations). Vertical velocities are taken from the weather model and do not include settling, and wind directions vary with altitude, but the maps give a general impression of wind direction. The start dates are (a) 15 April 2010, (b) 20 April 2010 and (c) 5 May 2010. During the most explosive phases of the eruption (Figures 1a and 1c), the wind direction was not directly toward the UK.

resulted in them being under-reported relative to silicic ones [Thordarson and Larsen, 2007]. Written records exist of ashfall in Europe for 8 eruptions in the last 400 years, and Thorarinsson [1981] compiled a number of contemporary reports. Wastegård and Davies [2009] summarize the characteristics of 18 widely occurring tephra layers on mainland Europe. They concluded that their distribution was patchy, with dispersal in many directions and along curved paths, making it difficult to predict where an individual tephra layer will be found.

[3] The April–May 2010 eruption of Eyjafjallajökull was only moderate in size and with low intensity [Gudmundsson et al., 2010, 2011]. Nevertheless, tephra from the eruption was carried to the European mainland, causing severe disruption to air traffic. The eruption was closely monitored and the ash cloud tracked by remote sensing (satellite, LiDAR) and modeled by dispersion models. The characteristics of the eruption and the meteorological conditions are consequently well constrained. Here we present a compilation of results of sampling and analysis of tephra from across Europe, especially the United Kingdom. These include estimates of timing, quantity and grain size distribution of tephra deposition and are discussed with respect to weather conditions and eruption characteristics. Measurements of the atmospheric concentration of particles with a diameter of  $<10\text{ }\mu\text{m}$  (PM10) at ground level are also presented. They indicate where very fine particles are likely to have been deposited, as well as being important to determine the hazard to health from the eruption [Horwell and Baxter, 2006].

## 2. Background

### 2.1. Eruption Characteristics

[4] The 2010 Eyjafjallajökull summit eruption lasted 39 days and erupted  $0.27 \pm 0.08\text{ km}^3$  tephra (uncompacted volume) in four distinct phases [Gudmundsson et al., 2010].

The first phase, from 14–18 April was characterized by explosive activity with a plume 5–10 km tall and a discharge rate of  $5–10 \times 10^5\text{ kg s}^{-1}$ . The majority of the tephra was erupted during this phase. Phase 2 (18 April–4 May) involved weak, strombolian-type, explosions and a low plume (2–4 km), accompanied by lava effusion. Explosive activity resumed on 5 May (Phase 3) with a plume  $>8\text{ km}$  high for the first two days and persisted at variable levels until 18 May, after which there was a period of declining explosivity (Phase 4) until the eruption ended on 22 May [Gudmundsson et al., 2010].

[5] The majority of the tephra was produced in two periods, 14–18 April (Phase 1) and 5–7 May (start of Phase 3). Fragmentation was efficient and 90% of grains had a diameter of  $<1\text{ mm}$  [Gudmundsson et al., 2010]. Despite this, most of the tephra was deposited near the volcano, with particle aggregation playing an important role in the premature deposition of fine-grained material [Taddeucci et al., 2011]. The total erupted mass of tephra, estimated from deposition maps and satellite data, was  $378 \pm 112\text{ Tg}$ , with 50% of this being deposited on land in Iceland [Gudmundsson et al., 2011; Gudmundsson, personal communication, 2012]. Using a combination of satellite data, plume height measurements and plume-rise models, Stohl et al. [2011] estimated that a total of  $8.3 \pm 4.3\text{ Tg}$  of material between  $2.8$  and  $28\text{ }\mu\text{m}$  was transported from Iceland in the plume.

### 2.2. Meteorology

[6] As far as European aviation is concerned, the weather conditions were a worst-case scenario. Leadbetter and Hort [2011] used the NAME dispersion model to simulate a small Hekla eruption every 3 hours using real weather data from the period 2003–2008 and found that the most likely transport direction was to the east. During the Eyjafjallajökull 2010 eruption, the wind had a northerly component for 71% of the eruption duration [Petersen et al., 2012]. Furthermore,

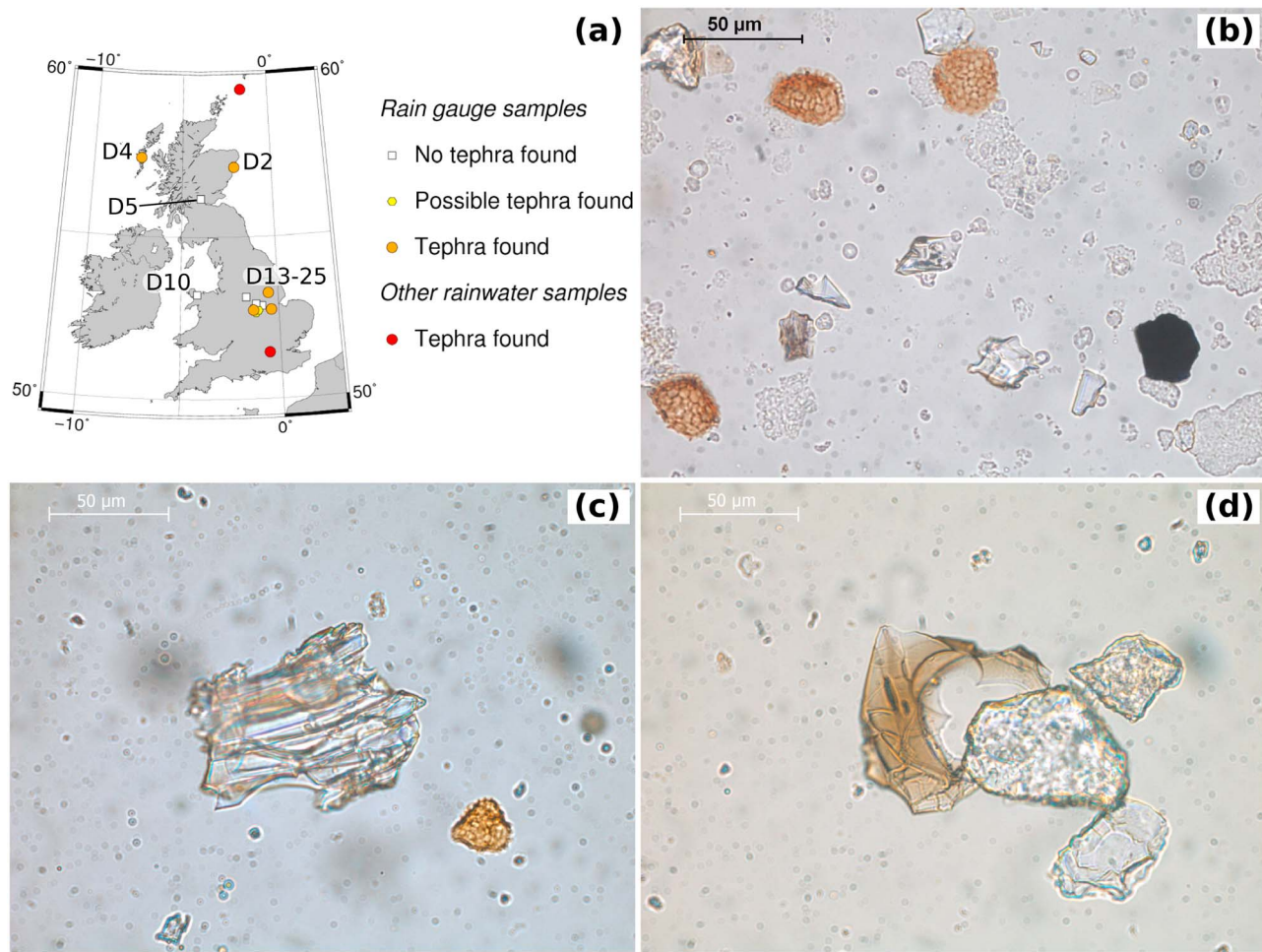


**Figure 2.** Results of rain gauge sampling. (a) Map of rain gauge tephra sample locations (see Table 1 for details) and example images of grains. The photomicrographs were taken in plane polarized light at 500 $\times$  magnification. (b) Two typical tephra grains. One grain is pale (center of image), the other is darker brown (lower left). The grains are 20–30  $\mu\text{m}$  in diameter, with sharp edges, and contain small bubbles and phenocrysts. The round orange objects, around 30  $\mu\text{m}$  in diameter, are spores of *Lycopodium clavatum*. Also present are many clear and opaque mineral grains. [Sample D14]. (c) A large, pale grain, with a diameter of over 100  $\mu\text{m}$ . It is vesicular, with tube-like vesicles. [Sample D17]. (d) A large, dark grain, with a diameter of  $\sim$ 80  $\mu\text{m}$ . It preserves the shape of large spherical bubbles. [Sample D17].

stable anticyclonic conditions resulted in low wind speeds and little precipitation, so ash was not advected away or washed out. Figure 1 shows example particle trajectories for 3 periods during the eruption, including the most explosive phases, that demonstrate transport toward Europe.

### 3. Rain Gauge Tephra Sampling in the UK

#### 3.1. Method

[7] Sampling kits similar to rain gauges, containing a plastic funnel (diameter: 150 mm, area 0.023  $\text{m}^2$ ) and a 2 litre plastic collecting bottle, were sent to volunteers across the UK (Figure 2a) by the British Geological Survey (BGS). They were set up on elevated platforms (0.25–1 m) in open areas (e.g. fields, gardens, roofs) away from roads or other local dust sources. The bottle was part-filled with deionized water to stop it blowing over. The funnel and bottle sampling kit were exposed for approximately 7 days at the end

of April or early May (Table 1). Each day, the funnel was rinsed into the bottle with deionized water to ensure that both wet- and dry-deposited tephra were collected. At the end of the sampling period, the bottles were sealed and returned for analysis.

[8] The samples were processed as follows: first, excess water was removed by evaporation over 10–15 days in a drying oven at 60°C, until the sample volume was <100  $\text{cm}^3$ . Large particle organic contamination (e.g. leaves, insects) was removed with a 150  $\mu\text{m}$  sieve. This organic material was mixed with 10% NaOH at 90°C for 15 min to loosen adhering particles, then the mixture was sieved again, with the filtrate being combined with the rest of the sample and the remaining organic material discarded. The rainwater was then centrifuged in a 15  $\text{cm}^3$  centrifuge tube until <2  $\text{cm}^3$  remained (repeated steps of 5 min at 3000 rpm). 30% H<sub>2</sub>O<sub>2</sub> was added to digest organic material and the samples were held in a hot-water bath at 90°C until the bubbling stopped,

**Table 1.** Results of Analysis of Rain Gauge Samples<sup>a</sup>

Sample	Location	Long. (°E)	Lat. (°N)	Sample Period	Tephra Present	Grain Size ( $\mu\text{m}$ )	Grain Count ( $\text{cm}^{-2}$ )
D2	Aberdeenshire	-2.10	57.15	11/05–20/05	Yes	33 ± 18	22
D4	Benbecula	-7.34	57.43	13/05–20/05	Yes	18 ± 7	218
D5	Perthshire	-3.97	56.18	12/05–20/05	No	—	—
D10	Anglesey	-4.16	53.22	22/04–28/04	No	—	—
D13	Leicestershire	-1.24	52.77	23/04–30/04	No	—	—
D14	Lincolnshire	-0.50	53.26	26/04–03/05	Yes	31 ± 15	9
D16	Nottinghamshire	-1.07	52.87	23/04–30/04	No	—	—
D17	Lincolnshire	-0.38	52.74	24/04–30/04	Yes	32 ± 22	8
D18	Leicestershire	-1.29	52.73	25/04–03/05	Yes	28 ± 9	179
D19	Leicestershire	-1.16	52.65	23/04–30/04	Maybe	—	—
D20	Derbyshire	-1.64	53.14	23/04–30/05	No	—	—
D21	Leicestershire	-0.85	52.87	23/04–30/04	No	—	—
D22	Leicestershire	-1.04	52.72	23/04–01/04	Maybe	—	—
D25	Nottinghamshire	-1.14	52.92	22/04–30/04	No	—	—
AM03*	Fair Isle	-1.64	59.52	16/04	Yes	25–55	—
AM27	Surrey	-0.57	51.42	16/04–19/04	Yes	~30	—
AM28	Surrey	-0.58	51.43	19/04	Yes	—	—
AM29	Surrey	-0.58	51.43	17/04–20/04	Yes	—	—
AM31	Surrey	-0.55	51.43	15/04–16/04	No	—	—
AM31	Surrey	-0.55	51.43	16/04–17/04	Maybe	—	—

<sup>a</sup>Sample AM03 was a surface swab of a window. Samples AM27–AM31 were collected in buckets.

typically after 1 hour. Each sample was rinsed with deionized water, centrifuged, and spiked with a tablet containing 18,500 spores of *Lycopodium clavatum*, which was dissolved using 10% HCl, then rinsed and centrifuged ( $\times 3$ ) again. The spores are easily recognized and are counted alongside the tephra grains to calibrate the results [e.g., Stockmarr, 1971]. This method is common practice in palynology research, but this is the first time that it has been used for tephra particles in rainwater. Finally, a few drops of the mixture were placed on a glass slide and allowed to dry, before Naphrax (a mountant with a high refractive index of 1.73) was used to attach the coverslip.

[9] Grains were counted using plane-polarized light at 500 $\times$  magnification on a petrological microscope. Counts were made along transects until at least 300 *Lycopodium* spores had been counted. Tephra grains were identified on the basis of their angular shape, isotropic structure, and the presence of bubbles and crystals within them (Figure 2c). It is difficult to identify grains with a diameter of  $<10 \mu\text{m}$  and these were not included in the counts. Microtephra concentrations are usually reported as grains per  $\text{cm}^3$  of sediment, so the counts were scaled to grains per  $\text{cm}^2$ , as though they had been deposited on an aggrading surface. A number of other rainwater samples from across the UK were also collected, using various containers (e.g. buckets). These were mounted and checked for the presence of tephra, but no counts were made (Table 1; samples AM27–31). A sample of 2010 tephra from the flanks of Eyjafjallajökull was dispersed in deionized water then processed and analyzed in the same manner, to act as a control.

[10] Scanning Electron Microscope (SEM) analysis was also used. Samples were prepared by drying drops of the concentrated tephra/*Lycopodium* mixture onto carbon stubs, before a carbon coating was applied. Energy Dispersive X-ray Spectroscopy (SEM-EDS) was used to make a semi-quantitative analysis of the composition of the grains. Sample spectra are plotted against the average spectrum of a number of spectra from the control, and the intensity is scaled so that the Si- $\text{k}\alpha$  peak is approximately the same for all samples.

This also allowed data from other labs e.g. Budapest, to be compared.

### 3.2. Results

[11] The results from the rain gauge samples are presented in Table 1 and show that tephra was deposited at many locations across the UK (Figure 2a). Mineral dust made up the majority of the grains in each of the samples and a small amount of organic material survived the preparation process. Two types of glass tephra grain were present: colorless and brown (Figure 2b). All were isotropic, most were angular and many contained bubbles and crystals.

[12] Grain counts relative to  $\sim 300$  *Lycopodium* spores correspond to 8–218 grains  $\text{cm}^{-2}$ . Small ( $<10 \mu\text{m}$ ), isotropic grains were present in all samples that contained tephra but could not be definitively identified as volcanic glass. The modal grain size of all counted grains was around 25  $\mu\text{m}$ , and most grains were below 45  $\mu\text{m}$  in diameter. A number of larger grains, up to 100  $\mu\text{m}$  were present, and these were always highly vesicular (Figures 2c and 2d). Aggregate clasts were also present (Figure 3a). Samples analyzed by SEM-EDS contained mineral grains (e.g. feldspar, quartz) and particles rich in metals (e.g. Fe, Pb, Sn). Glass tephra shards have peaks for Si, O, Al, Ca, Mg, Na, K, Fe, in good agreement with the control samples (Figure 3b). Aggregate clasts showed an additional peak for sulphur (S).

[13] There was no well-defined geographic trend in grain size or grain count. The modal grain size is  $\sim 25 \mu\text{m}$  everywhere in the UK, although much larger grains and aggregates could be found. Samples collected in central England at the end of April (D13–D25) have a large range in grain count (with only 50% of samples containing any tephra at all), suggesting that deposition was spatially patchy.

### 4. Dry Deposition of Aggregate Grains in the UK

[14] Tephra grains formed a dusty coating on cars and other surfaces in Leicestershire ( $\sim 1600$  km from the volcano) on the 19th, 21st and 24th April, and had not been observed prior to this. Samples were collected by ‘swabbing’ surfaces

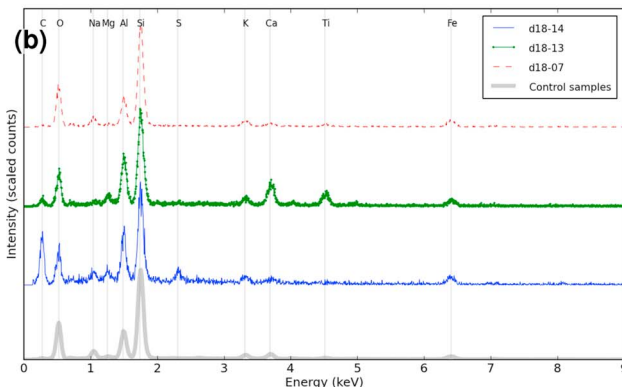
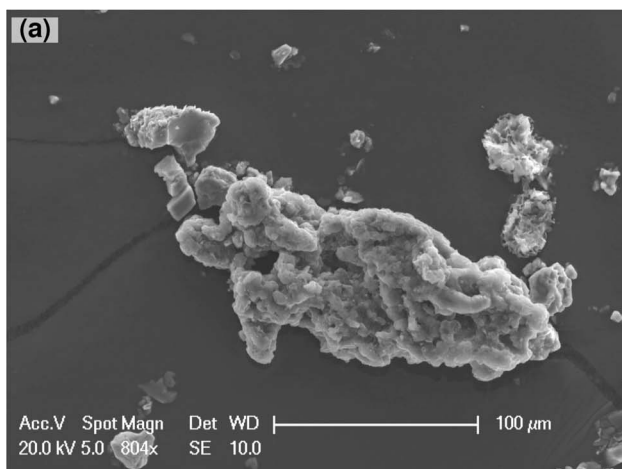


**Figure 3.** SEM analysis of particles from UK rain gauge samples. (a) Aggregate particle (Sample D18) deposited in Leicestershire during the second phase of the eruption. (b) SEM-EDS spectra for individual particles. There is good agreement with proximal control samples, and an extra peak for sulphur in the aggregate particles (e.g. d18-14).

with sticky tape, or by collectors made of double-sided sticky tape in petri dishes, and analyzed by SEM (Figure 4a).

[15] Aggregate grains ranged in diameter from 60–100  $\mu\text{m}$  on the 19th, 10–100  $\mu\text{m}$  on the 21st and 30–200  $\mu\text{m}$  on the 24th, with a mean of 85  $\mu\text{m}$ . The aggregate grains were well-cemented with irregular, angular, shapes and comprised smaller angular grains generally <5  $\mu\text{m}$  in diameter. They appeared to have a relatively low porosity. Some aggregates had well-formed crystals on their surfaces (possibly gypsum, halite or apatite), indicative of secondary mineralization [Gilbert and Lane, 1994]. Under SEM-EDS analysis, the same peaks were present as in the proximal control samples, but with an additional peak for sulphur (S; Figure 4b). This peak is further evidence of secondary mineralization e.g. by gypsum ( $\text{CaSO}_4 \cdot \text{H}_2\text{O}$ ).

## 5. Concentration of PM10 in the UK

### 5.1. Method

[16] Measurements of the airborne concentration of PM10 were collected by instruments from the Scottish Air Quality Database (SAQD; <http://www.scottishairquality.co.uk>) and

Department for Environment, Food and Rural Affairs' Automatic Urban and Rural Network (DEFRA AURN; <http://uk-air.defra.gov.uk>). The instruments used were either Tapered Element Oscillating Microbalance - Filter Dynamics Measurement System (TEOM-FDMS) or standard TEOMs that have had the loss of the volatile component of PM10 accounted for by using the Volatile Correction Model (TEOM-VCM) [Green *et al.*, 2009].

[17] The basic principle of operation of both the TEOM-FDMS and TEOM are identical. The ambient sample stream is first drawn through a size fractioning PM10 inlet which selects particles of the required aerodynamic cross-sectional diameter. This air stream, containing only PM10 particles, then passes through a Teflon filter which is attached to an oscillating tapered element. The PM10 is collected on the filter and the mass gained decreases the frequency of the

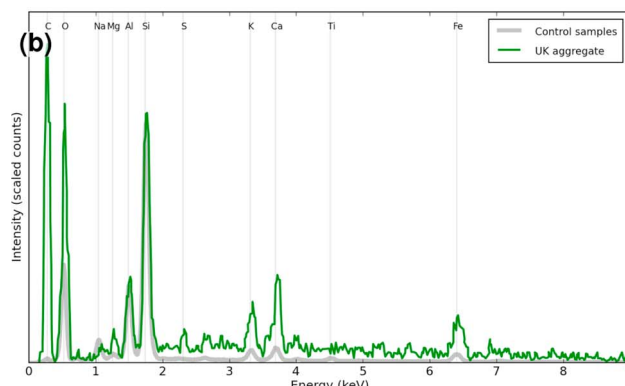
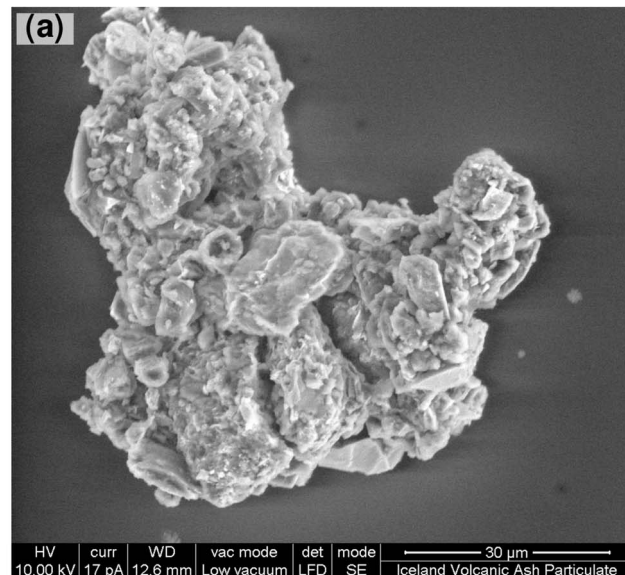


**Figure 4.** SEM analysis of an aggregate particle collected by sticky-tape sample in the UK. (a) Non-spherical, low porosity aggregate 60  $\times$  80  $\mu\text{m}$ , with component blocky particles <5  $\mu\text{m}$  wide (maximum 20  $\mu\text{m}$ ). This particle was collected in Leicestershire on 19 April 2010. (b) SEM-EDS data show good agreement with control samples and an additional sulphur (S) peak.

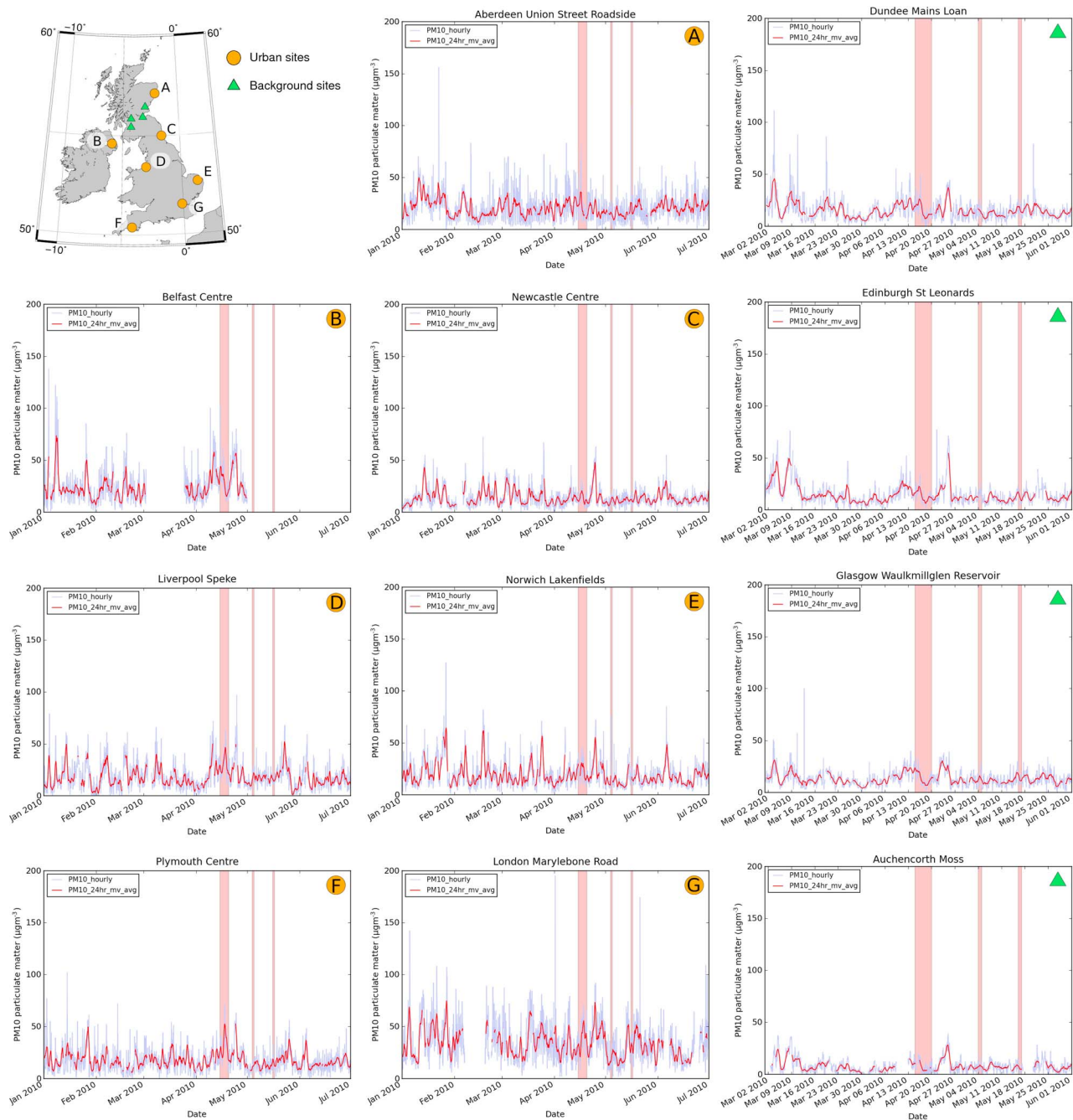


**Figure 5.** PM10 concentration data (hourly measurements and 24 hour moving average values) across the UK from the Scottish Air Quality Database (SAQD; “Background” sites, green triangles) and the Automatic Urban and Rural Network (AURN; Urban sites, orange circles). The data represent all parts of the country and cover the early part of 2010 to give context to background fluctuations. The red vertical bars indicate periods when UK airports were closed during the most explosive phases of the eruption (15–20 April, 4–5 May, 16–17 May). Although there are no significant peaks in surface concentration of PM10 at these times, there is a small rise in that 24-hour moving average at most stations across the UK during 21–24 April.

oscillating tapered element. By knowing the spring constant of the tapered element and by measuring this change of frequency, the mass gained by the filter can be calculated. This calculation is carried out automatically by the TEOM-FDMS or TEOM control unit. Both TEOM-FDMS and

TEOM-VCM data have been found to be equivalent to the European Union’s reference method for monitoring PM10. All instruments in the SAQD and AURN undergo extensive 6-monthly QAQC audits and the data are subjected to a detailed ratification process by AEA.

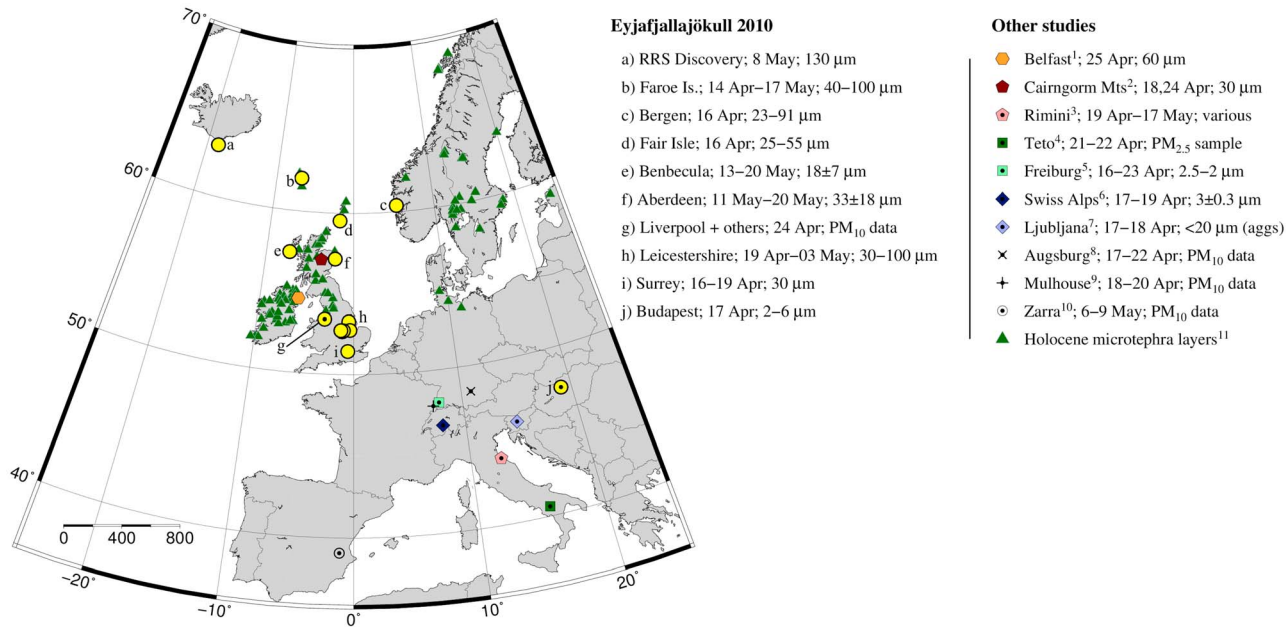


**Figure 6.** Map of Icelandic tephra deposition in Europe. Locations where Eyjafjallajökull tephra was found at ground level in this and other studies are marked. Sample collection dates are given, but tephra may also have fallen at other times. Symbols containing black dots represent samples collected by air quality monitoring equipment. Tephra collected by air quality monitoring equipment extend the range to over 3000 km. Sources: 1. Davies *et al.* [2010], 2. Dawson *et al.* [2011], 3. Rossini *et al.* [2012], 4. Lettino *et al.* [2012], 5. Schleicher *et al.* [2012], 6. Bukowiecki *et al.* [2011], 7. Gao *et al.* [2011], 8. Pitz *et al.* [2011], 9. Colette *et al.* [2011], 10. Revuelta *et al.* [2012], 11. Holocene microtephra layers from Swindles *et al.* [2011] are plotted for comparison.

[18] Steps were taken to ensure that data are representative. Instruments situated at “background” sites were located away from significant anthropogenic sources. Diurnal fluctuations at these sites tend to be small, so their data are often helpful in detecting wide-ranging pollution episodes and also for short term transient events. Short term transient events may not be visible in the data from sites that are located close to anthropogenic sources, such as roadside locations, as diurnal fluctuations at such sites can be much greater. It is usual for PM<sub>10</sub> concentrations at all site types to vary from day-to-day, these variations can be caused by various factors such as anthropogenic activity and air mass back trajectories. It is therefore important to look at data from a number of sites and over a long time span to give context to individual results.

[19] For the purposes of this discussion, increased PM<sub>10</sub> concentrations within the boundary layer are assumed to mean that tephra was being deposited at this point. PM<sub>10</sub> concentrations at higher altitudes may have been greater or less at these times.

## 5.2. Results

[20] Figure 5 shows PM<sub>10</sub> results from a number of sites across the UK. Data from a six month period from January–July are plotted to illustrate the level of diurnal variations. The periods of airport closures, which correspond to the most explosive phase of the eruption are also plotted (15–20 April, 4–5 May, 16–17 May). Most sites have continuous data throughout the duration of the eruption. In all locations, the baseline concentration is generally <50 µg m<sup>-3</sup>. The levels

fluctuate by ~50 µg m<sup>-3</sup> at the urban sites, and by ~25 µg m<sup>-3</sup> at the background sites.

[21] During the eruption, no locations recorded PM<sub>10</sub> levels that were significantly outside the six-monthly range of the fluctuations. On 21–24 April, the 24-hour moving average data show a period when PM<sub>10</sub> levels are higher than the six-month average by ~20 µg m<sup>-3</sup>. Although the increase is small, the signal can be seen simultaneously in stations across the whole of the UK (except Aberdeen). In each location the peak builds gradually then drops sharply. For such a large area to be affected, and at a time when air mass trajectories lead from Iceland (Figure 1b), this increase is probably due to volcanic ash. During this period, the hourly mean PM<sub>10</sub> concentration in Liverpool reached nearly 100 µg m<sup>-3</sup>.

## 6. Other Observations of Tephra Deposition Across Europe

### 6.1. Wet and Dry Deposition

[22] Tephra was also collected at a number of other sites outside Iceland (Figure 6). It was deposited upon the research ship Discovery (cruise D350), 75 km SE of the volcano (63.108°N, -18.611°E) between 15:54 hrs and 17:12 hrs on 8 May 2010. The mass-loading was 34 g m<sup>-2</sup> ± 50%, and the modal grain size was 130 µm. Analysis of rainwater that fell in Tórshavn, Faroe Islands (62.01°N, -6.79°E) over the period 14 April to 17 May gives a mass loading of 0.6 g m<sup>-2</sup>. Sufficient material was present to measure the grain size distribution by Coulter counter. The

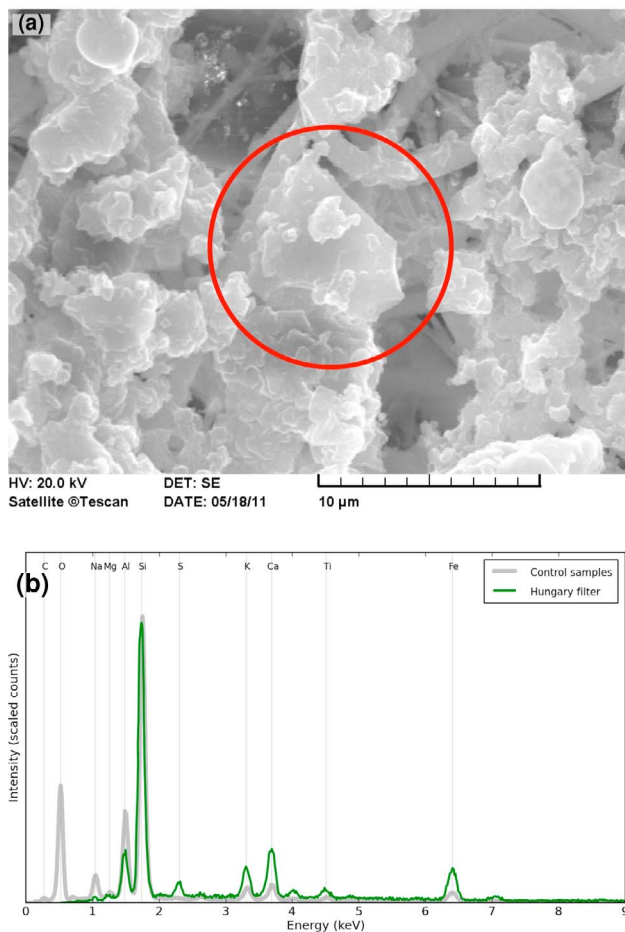


**Figure 7.** Eyjafjallajökull tephra from Budapest, Hungary. (a) SEM Secondary Electron image of tephra grain, approximately 6  $\mu\text{m}$  in diameter. The sharp, curved edges are consistent with tephra formed from bubbly magma. (b) SEM-EDS spectrum data show good agreement with control samples and an additional sulphur (S) peak.

modal grain size was 40  $\mu\text{m}$ , although grains of up to 100  $\mu\text{m}$  were present. Grains of both pale, shandy and brown, equant types were present, as were aggregates containing grains <10  $\mu\text{m}$  diameter. Rainwater falling in Bergen, Norway (60.39°N, 5.33°E) on 16 April contained grains that were identifiable by optical microscope. They ranged from 23–91  $\mu\text{m}$  in diameter (mean 48  $\mu\text{m}$ ), with both pale and dark types present. Tephra was also present in rainwater in Bergen on 23 April.

## 6.2. Air Filtering

[23] Tephra was collected on an air filter in Budapest, Hungary (47.47°N 19.05°E, ~3000 km from the volcano) on 17 April, which coincided with the detection of volcanic ash above Hungary in Eumetsat data (<http://oiswww.eumetsat.org/IPPS/html/MSG/RGB/DUST/CENTRALEUROPE/index.htm>). The grains were identified by SEM and were 2–4  $\mu\text{m}$  in diameter (maximum 6  $\mu\text{m}$ , Figure 7a). Under SEM-EDS analysis, the spectrum had the same peaks for Si, Al, Ca, Fe, K that are found with proximal samples. An extra peak

corresponding to S may result from precipitation of sulphate minerals on the surface of the grain during transport (Figure 7b). Peaks in surface PM10 concentration were detected in Budapest and Nyíregyháza of 80 and 120  $\mu\text{g m}^{-3}$ , respectively, also on 17 April 2010. However, such peaks are within the levels of normal fluctuations and cannot definitively be attributed to volcanic ash.

## 7. Discussion

### 7.1. Eruption Rate, Weather and Dispersal

[24] Tephra was deposited in Europe in each of the first three phases of the eruption. Phase 1 (14–18 April) was most powerful and produced the highest plume (12 km), with an estimated discharge rate of  $5–10 \times 10^5 \text{ kg/s}$  [Gudmundsson et al., 2011; Gudmundsson, personal communication, 2012]. Stohl et al. [2011] estimated fine material subject to long-range transport was produced at  $0.4–0.8 \times 10^5 \text{ kg/s}$ . During this period the wind blew toward the south east down the east side of the UK (Figure 1a) carrying tephra to Norway, and to central Europe, where it was detected by air filters and increased PM10 concentrations. In the UK, tephra was deposited in the Fair Isle and possibly in Surrey, but there was no widespread increase in PM10 concentration during this time.

[25] The plume height and discharge were much lower during Phase 2 (4–10 km and  $0.05–0.9 \times 10^5 \text{ kg/s}$ ) [Gudmundsson et al., 2011; Gudmundsson, personal communication, 2012], but tephra was collected in the UK in rain gauge and sticky-tape samples. There was a small but widespread increase in PM10 concentrations. During this period, air mass trajectories pass directly over the UK from Iceland (Figure 1b). This highlights the importance of wind direction in controlling the distribution of tephra. PM10 concentrations remained elevated in some parts of Europe (Figure 6).

[26] During Phase 3 (5–18 May), the plume height and discharge rate increased and was highly variable (4–10 km and  $0.3–4 \times 10^5 \text{ kg/s}$ ) [Gudmundsson et al., 2011; Gudmundsson, personal communication, 2012], while air mass trajectories from the volcano pointed due south (Figure 1c). Tephra was deposited in Benbecula in the UK but PM10 concentrations were normal across the country. On mainland Europe, Revuelta et al. [2012] noted elevated sulphate levels across Spain from 4–16 May. In particular, above-average PM10 concentrations were recorded in Zarza, Valencia from 6–9 May.

### 7.2. Tephra Characteristics

[27] The grain counts of the rain gauge samples ( $8–218 \text{ grains cm}^{-2}$ ) are similar to measurements from micro-tephra layers. Although the mean discharge was lower, the erupted volume of the Eyjafjallajökull 2010 summit eruption was comparable to Hekla 1947 ( $0.2 \text{ km}^3$  fresh-fallen tephra [Thorarinsson, 1970]), which deposited 20  $\text{grains cm}^{-3}$  of sediment in Northern Ireland [Swindles et al., 2010]. Deposits from the Hekla 1104 eruption ( $2 \text{ km}^3$  [Larsen and Eiriksson, 2008]) in Ireland contain around 300  $\text{grains cm}^{-3}$  [Wastegård and Davies, 2009]. The loading of 179  $\text{grains cm}^{-2}$  in Leicester (Sample 18) is high considering that it was produced during Phase 2 of the eruption. This may indicate that even small plumes can produce relatively high grain counts in localized areas. This implies that the eruptions that

produced tephra layers for which the source is not known do not need to have been very large, and is in agreement with the conclusions of *Dugmore et al.* [1996], who identified tephra from the relatively small A.D. 1510 Hekla eruption within the UK. Alternatively, the high grain count of D18 may indicate that the preservation of older microtephras was incomplete.

[28] Some of the largest particles deposited in the UK were aggregates with diameters up to 200  $\mu\text{m}$ . This is smaller than the aggregate grains that fell in Iceland (250–1500  $\mu\text{m}$  [*Taddeucci et al.*, 2011]). The component grains are 1–10  $\mu\text{m}$  in diameter, which is too small to be identified by optical microscope. It is also much smaller than the component grains of the aggregates that fell close to the volcano (mostly 63–250  $\mu\text{m}$  [*Taddeucci et al.*, 2011]), which may indicate that the distal aggregates formed in a different part of the plume. If aggregate clasts in microtephra layers have disintegrated into grains smaller than 10  $\mu\text{m}$ , they are likely to be missed during analysis, which will lead to underestimation of the mass loading if the microtephra layer contained a significant proportion of aggregate clasts.

### 7.3. Extending the Known Dispersion Range of Icelandic Tephra

[29] Holocene Icelandic microtephra layers are mainly found in the UK and Scandinavia [*Swindles et al.*, 2011], and the Vedde ash (Younger Dryas age) has been identified in southern Germany and Switzerland [*Blockley et al.*, 2007]. Tephra grains with similar compositions to known Icelandic eruptions have also been identified in ice cores from Greenland [*Zielinski et al.*, 1997].

[30] Prior to the Eyjafjallajökull 2010 eruption, the most distal reported tephra fallout from an Icelandic eruption was in Helsinki, Finland, around 52 hours after the onset of the Hekla 1947 eruption [*Thorarinsson*, 1981]. During the Eyjafjallajökull 2010 eruption, air quality monitoring equipment at ground level allowed collection of tephra grains from much more distal locations (Figure 6) such as Hungary, southern Germany [*Schleicher et al.*, 2012], Switzerland [*Bukowiecki et al.*, 2011], Slovenia [*Gao et al.*, 2011] and Italy [*Lettino et al.*, 2012; *Rossini et al.*, 2012] at distances of >3000 km from Iceland, thus extending the known range of Icelandic tephras. Unfortunately, the small size of the distal grains (2–10  $\mu\text{m}$ ) would make them very difficult to find as microtephras, and identification would only be possible by expensive and time-consuming techniques such as SEM and electron microprobe.

[31] The tephra grains collected from air filters are very small, but coarser material may have been missed in these locations by equipment designed to only sample particles smaller than 10  $\mu\text{m}$  in diameter. *Rossini et al.* [2012] used a sampler without an upper size limit 19 April–17 May in Rimini, Italy (2900 km from the volcano), and found the modal grain size of volcanic particles was 44–63  $\mu\text{m}$ . This is surprising because it is much coarser than samples from much closer to the volcano (e.g. the UK), and because settling calculations based on Stokes' law suggest that 50  $\mu\text{m}$  grains should be deposited around 1500 km from the vent. Because most of the particles that they identified as volcanic were crystals of common minerals (e.g. pyroxene) and because the glass shards were not compared with proximal

tephras, it is probable that many of these grains have a more local source than Eyjafjallajökull.

### 7.4. Estimates of Airborne Tephra Concentration

[32] The grain size of the tephra in the rain gauge samples (commonly 25  $\mu\text{m}$ , with some >100  $\mu\text{m}$ ) is coarser than optimal range for most airborne ash concentration measurement techniques. Large grains are filtered out by many types of air quality monitoring equipment. While these grains are less hazardous to health than finer material [*Horwell and Baxter*, 2006], this means that using PM10 data alone can underestimate the concentration of airborne tephra. Furthermore, detection of volcanic ash in satellite data (e.g. Advanced Very High Resolution Radiometer; AVHRR) using the brightness temperature difference method is only possible with the finest ash grain sizes (with a dominant effective radius of <17  $\mu\text{m}$  [*Wen and Rose*, 1994]). High concentrations of coarse particles will make the cloud appear opaque, but at lower concentrations the potential presence of coarser particles adds a further source of uncertainty to estimates of ash concentration.

## 8. Conclusion

[33] Tephra from the 2010 summit eruption of Eyjafjallajökull was transported far from Iceland. Tephra from the first phase of the eruption was carried southeastward into central Europe. The second phase mainly deposited tephra in the UK. Tephra from the third phase was carried south of Iceland toward Spain. Glass shards collected in the UK and Scandinavia have a similar distribution to Holocene microtephra layers. They were typically 20–50  $\mu\text{m}$  in diameter, but larger grains were also present. Aggregate clasts deposited in the UK had a mean diameter of 85  $\mu\text{m}$  and show evidence for cementation by sulphur-rich minerals. Air filters and PM10 detectors allowed detection of tephras at ranges of >3000 km from the volcano. These results demonstrate that even a moderately sized Icelandic eruption can deposit tephra over a significant proportion of Europe.

[34] **Acknowledgments.** The authors are grateful to all the volunteers who collected tephra samples and sent them in for analysis. Julian Bukits, Aoife O'Mongain, Simon Chinery, and Kay Green (British Geological Survey) organized the rain gauge sampling. This work is published by permission of the Executive Director, British Geological Survey (NERC). Anthony Newton and Andy Dugmore (Edinburgh University) are thanked for useful advice on processing of rainwater samples. J.A.S. is funded by the Scottish Government and Marie Curie Actions via a Royal Society of Edinburgh personal research fellowship. The authors gratefully acknowledge the NOAA Air Resources Laboratory (ARL) for the provision of the HYSPLIT transport and dispersion model and READY website (<http://www.arl.noaa.gov/ready.php>) used in this publication.

## References

- Blockley, S., C. Lane, A. Lotter, and A. Pollard (2007), Evidence for the presence of the Vedde ash in central Europe, *Quat. Sci. Rev.*, 26(25–28), 3030–3036, doi:10.1016/j.quascirev.2007.09.010.
- Bukowiecki, N., et al. (2011), Ground-based and airborne in-situ measurements of the Eyjafjallajökull volcanic aerosol plume in Switzerland in spring 2010, *Atmos. Chem. Phys.*, 11(19), 10,011–10,030.
- Colette, A., et al. (2011), Assessing in near real time the impact of the April 2010 Eyjafjallajökull ash plume on air quality, *Atmos. Environ.*, 45(5), 1217–1221, doi:10.1016/j.atmosenv.2010.09.064.
- Davies, S. M., G. Larsen, S. Wastegård, C. S. M. Turney, V. A. Hall, L. Coyle, and T. Thordarson (2010), Widespread dispersal of Icelandic tephra: How does the Eyjafjöll eruption of 2010 compare to past Icelandic events?, *J. Quat. Sci.*, 25(5), 605–611, doi:10.1002/jqs.1421.

- Dawson, J., E. Delbos, R. Hough, D. Lumsdon, B. Mayes, and H. Watson (2011), Impacts of volcanic ash originating from the eruption in Eyjafjallajökull (Iceland) on the natural resources of Scotland, report, Macaulay Land Use Res. Inst., Aberdeen, U.K. [Available at <http://www.macaulay.ac.uk/policyrelevance/consultationresponses/2011/MLURI-response-to-volcanic-ash-impacts.pdf>.]
- Dugmore, A., A. Newton, K. Edwards, G. Larsen, J. Blackford, and G. Cook (1996), Long-distance marker horizons from smallscale eruptions: British tephra deposits from the AD 1510 eruption of Hekla, Iceland, *J. Quat. Sci.*, 11(6), 511–516.
- Gao, F., et al. (2011), Monitoring presence and streaming patterns of Icelandic volcanic ash during its arrival to Slovenia, *Biogeosci. Discuss.*, 8(2), 3863–3898.
- Gilbert, J. S., and S. J. Lane (1994), The origin of accretionary lapilli, *Bull. Volcanol.*, 56(5), 398–411, doi:10.1007/s004450050048.
- Green, D. C., G. W. Fuller, and T. Baker (2009), Development and validation of the volatile correction model for PM10: An empirical method for adjusting TEOM measurements for their loss of volatile particulate matter, *Atmos. Environ.*, 43(13), 2132–2141, doi:16:j.atmosenv.2009.01.024.
- Gudmundsson, M. T., et al. (2010), The April 2010 eruption of the ice-capped Eyjafjallajökull, South Iceland, paper presented at EGU General Assembly, Eur. Geosci. Union, Vienna.
- Gudmundsson, M. T., Á. Höskuldsson, G. Larsen, T. Thordarson, B. Oddsson, T. Hognadottir, I. Jónsdóttir, H. Björnsson, G. N. Petersen, and E. Magnússon (2011), Eyjafjallajökull April–June 2010: An explosive-mixed eruption of unusually long duration, *Geophys. Res. Abstr.*, 13, EGU2011-12542.
- Horwell, C., and P. Baxter (2006), The respiratory health hazards of volcanic ash: A review for volcanic risk mitigation, *Bull. Volcanol.*, 69(1), 1–24.
- Larsen, G., and J. Eiriksson (2008), Holocene tephra archives and tephrochronology in Iceland: A brief review, *Jökull*, 58, 229–250.
- Leadbetter, S. J., and M. C. Hort (2011), Volcanic ash hazard climatology for an eruption of Hekla Volcano, Iceland, *J. Volcanol. Geotherm. Res.*, 199(3–4), 230–241, doi:10.1016/j.jvolgeores.2010.11.016.
- Lettino, A., R. Caggiano, S. Fiore, M. Macchiatto, S. Sabia, and S. Trippetta (2012), Eyjafjallajökull volcanic ash in southern Italy, *Atmos. Environ.*, 48, 97–103, doi:10.1016/j.atmosenv.2011.05.037.
- Petersen, G. N., H. Björnsson, and P. Arason (2012), The impact of the atmosphere on the Eyjafjallajökull 2010 eruption plume, *J. Geophys. Res.*, 117, D00U07, doi:10.1029/2011JD016762.
- Pitz, M., J. Gu, J. Soentgen, A. Peters, and J. Cyrys (2011), Particle size distribution factor as an indicator for the impact of the Eyjafjallajökull ash plume at ground level in Augsburg, Germany, *Atmos. Chem. Phys.*, 11(17), 9367–9374, doi:10.5194/acp-11-9367-2011.
- Revuelta, M., M. Sastre, A. Fernández, L. Martín, R. García, F. Gómez-Moreno, B. Artíñano, M. Pujadas, and F. Molero (2012), Characterization of the Eyjafjallajökull volcanic plume over the Iberian Peninsula by lidar remote sensing and ground-level data collection, *Atmos. Environ.*, 48, 46–55, doi:10.1016/j.atmosenv.2011.05.033.
- Rossini, P., et al. (2012), April–May 2010 Eyjafjallajökull volcanic fall-out over Rimini, Italy, *Atmos. Environ.*, 48, 122–128, doi:10.1016/j.atmosenv.2011.05.018.
- Schleicher, N., U. Kramar, V. Dietze, U. Kaminski, and S. Norra (2012), Geochemical characterization of single atmospheric particles from the Eyjafjallajökull volcano eruption event collected at ground-based sampling sites in Germany, *Atmos. Environ.*, 48, 113–121, doi:10.1016/j.atmosenv.2011.05.034.
- Stockmarr, J. (1971), Tablets with spores used in absolute pollen analysis, *Pollen Spores*, 13, 615–621.
- Stohl, A., et al. (2011), Determination of time- and height-resolved volcanic ash emissions and their use for quantitative ash dispersion modeling: The 2010 Eyjafjallajökull eruption, *Atmos. Chem. Phys.*, 11(9), 4333–4351, doi:10.5194/acp-11-4333-2011.
- Swindles, G., F. De Vleeschouwer, and G. Plunkett (2010), Dating peat profiles using tephra: stratigraphy, geochemistry and chronology, *Mires Peats*, 7, 1–9.
- Swindles, G. T., I. T. Lawson, I. P. Savov, C. B. Connor, and G. Plunkett (2011), A 7000 yr perspective on volcanic ash clouds affecting northern Europe, *Geology*, 39(9), 887–890, doi:10.1130/G32146.1.
- Taddeucci, J., P. Scarlato, C. Montanaro, C. Cimarelli, E. Del Bello, C. Freda, D. Andronico, M. Gudmundsson, and D. Dingwell (2011), Aggregation-dominated ash settling from the Eyjafjallajökull volcanic cloud illuminated by field and laboratory high-speed imaging, *Geology*, 39(9), 891–894, doi:10.1130/G32016.1.
- Thorarinsson, S. (1970), *Hekla: A Notorious Volcano*, Almenna Bókafelagid, Reykjavík.
- Thorarinsson, S. (1981), Greetings from Iceland: Ash-falls and volcanic aerosols in Scandinavia, *Geogr. Ann., Ser. A*, 63(3–4), 109–118.
- Thordarson, T., and G. Larsen (2007), Volcanism in Iceland in historical time: Volcano types, eruption styles and eruptive history, *J. Geodyn.*, 43(1), 118–152, doi:10.1016/j.jog.2006.09.005.
- Wastegård, S., and S. M. Davies (2009), An overview of distal tephrochronology in northern Europe during the last 1000 years, *J. Quat. Sci.*, 24(5), 500–512, doi:10.1002/jqs.1269.
- Wen, S., and W. I. Rose (1994), Retrieval of sizes and total masses of particles in volcanic clouds using AVHRR bands 4 and 5, *J. Geophys. Res.*, 99(D3), 5421–5431, doi:10.1029/93JD03340.
- Zielinski, G. A., P. A. Mayewski, L. D. Meeker, K. Grönvold, M. S. Germani, S. Whitlow, M. S. Twickler, and K. Taylor (1997), Volcanic aerosol records and tephrochronology of the Summit, Greenland, ice cores, *J. Geophys. Res.*, 102(C12), 26,625–26,640, doi:10.1029/96JC03547.